

EVALUATION FOR ASR-INDUCED DEGRADATION THROUGH FEM SIMULATIONS

Kyushu Institute of Technology, Japan
Kyushu Institute of Technology, Japan
Sumitomo Osaka Cement Co., Ltd.

Doctoral Student, Yulong ZHENG
JPCEA Member, Professor, Kenji KOSA
Nobuo UEHARA

Abstract: Using specimens which simulated ASR, experimental tests and FEM analysis are performed to study characteristic of external degradation. Through experiment and analysis, both the ASR-induced circular deformation of concrete have been confirmed. From analysis results, the generation of circular and uniform deformation is caused by the component of bending and uniform tension effect in central cracks of profile. Due to the opening deformation of stirrup, great strain as 0.023 occurs in bent part of stirrup. This will promote the progress of initial damage, which will further cause rupture of stirrup as confirmed by experiment.

Keywords: ASR, Experiment, FEM Analysis, Circular Deformation, Rupture of Stirrup.

1. INTRODUCTION

For recent years, due to the Alkali Silica Reaction, (ASR for short), many concrete structures suffered degradations. It is reported that the bended part of reinforcing stirrups in bridge pier are frequently ruptured¹⁾. Due to the rupture of stirrup, poor anchorage occurs which will generate influence on bearing capacities of structures. In investigations, it is very effective if the possibility of rupture can be judged from the state of external degradation. However, induced by the inner expansion, the characteristics of external deformations and cracks, and their possible influences on rupture of stirrup are still not clear.

Therefore, concentrating on the effect from ASR expansion on stirrups and degradations of external concrete, experimental tests simulating ASR are performed. Specimens with expansive mortar cast into the frame surrounded by ordinary concrete are made. For contrasting with experiment, FEM analysis is also conducted.

In this paper, the authors will study the features of external deformations from inner expansion through the comparison of experiment and analysis. After that, the crack conditions will be compared and the connection with external deformations will also be evaluated. Further, the possible influence on behavior of stirrup from external degradations will be estimated.

2. EXPERIMENTAL AND ANALYTICAL CONDITIONS

Fig. 1 illustrates the shapes and reinforcements of specimen. For sake of simulating the effect from inner ASR expansion on external degradations and stirrups, the expansive mortar is cast in the square hollow part surrounded by the ordinary concrete as the frame. The external size is 680mm×680mm×1340mm with cross section as 1/4 to that of the actual bridge pier with stirrups ruptured. Further, the dimension of expansive mortar is set as 456mm×456mm. The spacing of stirrups is 285mm with stirrup ratio as 0.22% same with the actual bridge pier.

In addition, the shape of cross section is shown in Fig. 1-(c). Details for different rebar types can be referred to former research²⁾. The stirrup uses SD295 rebar with diameter as 16mm. Further, the thickness of covering concrete is 42mm. Mix proportion used for the frame concrete and expansive mortar is illustrated in Table 1 and Table 2, respectively.

The strength of frame concrete is 27N/mm² being the design strength for the actual bridge pier. By cylinder tests, the real strength is obtained as 35N/mm². Besides, the expansive agent is set as 200kg/m³ to induce the severe degradation condition.

The 2-dimensional elastic-plastic finite element analysis is conducted. The whole section is used for modeling as presented in Fig. 2-(a). The expansive mortar with the size

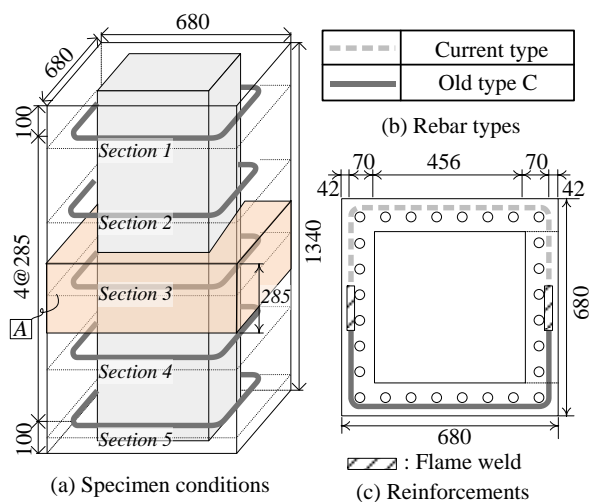


Fig. 1 Specimen Condition

as 456mm×456mm is simulated. As shown in Fig. 1-(a), the spacing of stirrups for section 2~4 is same as 285mm. Thus, for modeling these three sections, one stirrup is input into the model and with depth of the concrete model as 285mm (refer to A of Fig. 1-(a) for image, section 3 for instance). Based on observations from experiment, expansion in axial direction is confirmed. Therefore, plane stress elements considering strain in three directions are applied. The detail of model for the bended part of stirrup is presented in Fig. 2-(c). Same with the experiment, stirrup diameters is 16mm. Besides, the bending radius is 1.0 times of diameter, which has been confirmed to produce much initial damage on stirrups³⁾.

Fig. 3-(a) presents the stress-strain model of frame concrete. In compression side, the para-curve is developed until the compressive strength as 35N/mm². The Drucker-Prager criterion is used for the biaxial compressive situation. With respect to the tensile side, the curve grows in linear to the tensile strength. Then considering the softening condition, 1/4 model is used after the cracking. In addition, the Rankine criterion is applied for the biaxial tensile and tensile-compressive situations. Fig. 3-(b) describes the stress-strain model for stirrup. The yield and tensile strength is based on the values obtained by tensile test according to the JIS Z 2242 experiment method²⁾. Besides, Von-Mises criterion is adopted.

It is known that the expansive strain is influenced by restraint degree greatly. The free expansive strain is supposed to be ϵ_0 . In the restraint condition, the expansive strain ϵ_r will become smaller than ϵ_0 . The difference ($\epsilon_0 - \epsilon_r$) is considered to be saved. Thus, for getting the material model of expansive mortar, the relation between ($\epsilon_0 - \epsilon_r$) and compressive stress σ_c is necessary.

Due to the equilibrium of forces in steel and expansive mortar, the relation between free and restraint strain ϵ_0 , ϵ_r are obtained as Eq. 1:

$$\epsilon_r = \frac{E_c}{pE_s + E_c} \epsilon_0 \quad (1)$$

Herein, the E_s , E_c is the elastic modulus for steel and concrete and is assumed as $2.1 \times 10^5 \text{N/mm}^2$ and $2.78 \times 10^4 \text{N/mm}^2$, respectively. p is the steel ratio. Along with the process of expansion, the expansive mortar surfs

Table 1 Mix Proportion of Frame Concrete

G _{max} (mm)	W/C (%)	s/a (%)	Unit (kg/m ³)				Admixture
			W	C	S	G	
20	46	43	175	381	718	1018	1.142

Design strength: 27N/mm²

Table 2 Mix Proportion of Expansive Mortar

W/C (%)	Unit (kg/m ³)			
	W	C	S	Expansion Agent
40	231	575	1150	200

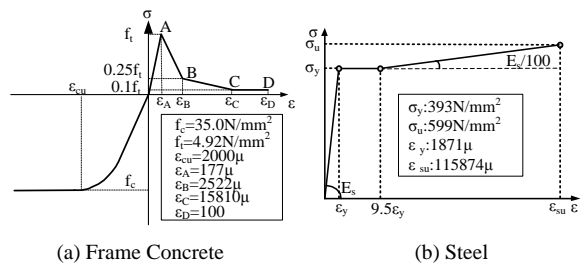


Fig. 3 Material Model

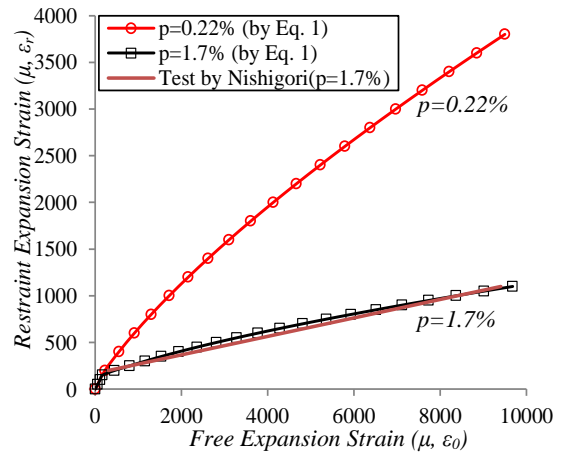


Fig. 4 Restraint & Free Expansive Strain

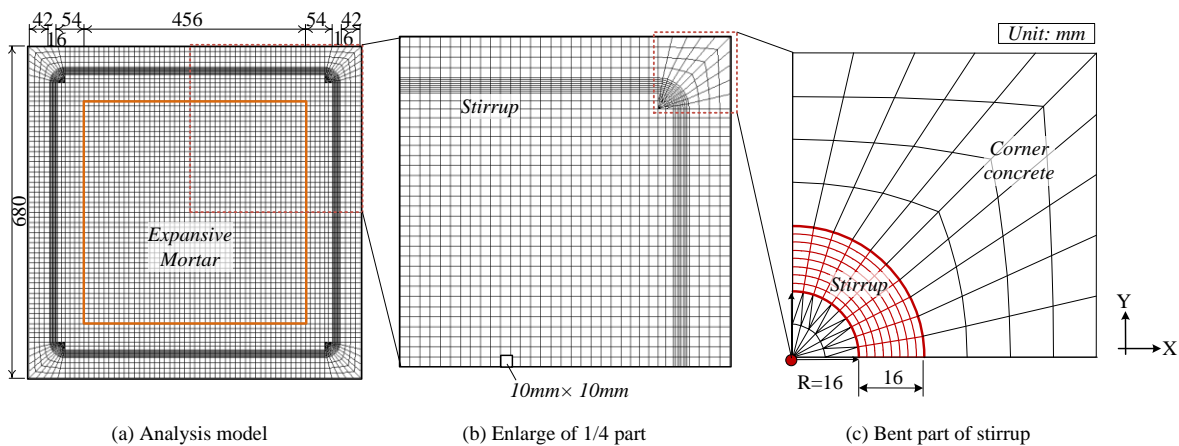


Fig. 2 Analysis Model

degradation and the young's modulus is considered to decrease. Thus, refer to the former research ⁴⁾, damage parameter, considering the decrease of young's modulus together with expansion, is imported into the young's modulus. As shown in Fig. 4, the test results are referred from Nishigori ⁵⁾ (p=1.7%) in uniaxial condition based on the standard method by JSCE. The rough coincidence between the test results and the calculated curve shows reasonability of the equation.

Thus, using the curve of p=0.22% same with specimen, relation between free and restraint strain is obtained. Fig. 5 shows the assumed expansive model, with stress-strain relation decided by Eq. 2:

$$\sigma_c = E_c \cdot (\varepsilon_0 - \varepsilon_r) \quad (2)$$

Besides, to produce expansion, temperature is input linearly to the expansive mortar, as the linear increase of temperature inner specimen was confirmed by experiment. The coefficient of expansion is set as $10^{-5}/^{\circ}\text{C}$ and 10°C is input for each step.

3. EVALUATION FOR EXTERNAL DEGRADATIONS

3.1 Deformation Conditions

In this section, external deformations of specimen from experiment and analysis are compared. Fixed steel frame is set around the specimen in experiment. Depth gauges are settled to measure the length from fixed frame to concrete surface. By calculating the difference of lengths before and after expansion, the deformation can be obtained. As illustrated in Fig. 6, for simplicities, the deformations are divided by two types as uniform deformation and circular deformation. Uniform

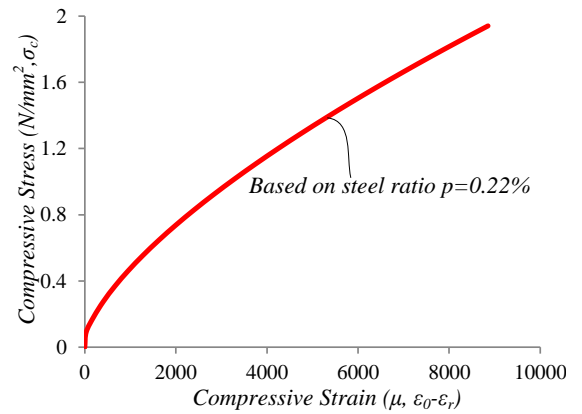


Fig. 5 Assumed Expansive Model

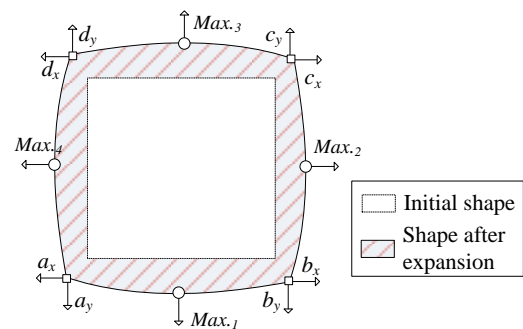
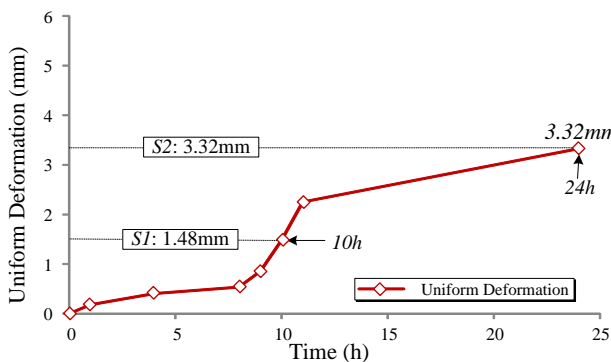
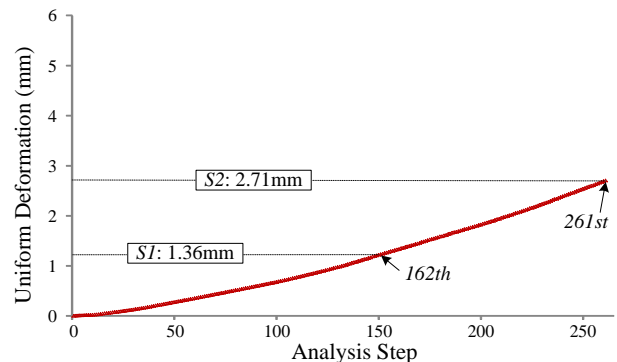


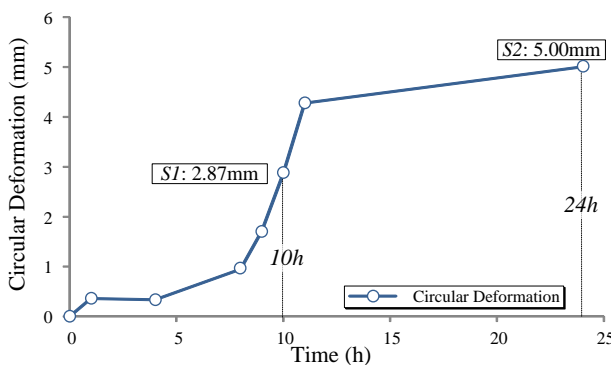
Fig. 6 Uniform & Circular Deformation



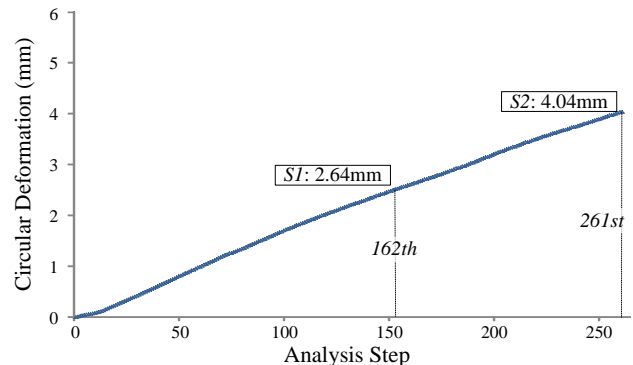
(a) Uniform Deformation (Experiment)



(b) Uniform Deformation (Analysis)



(c) Circular Deformation (Experiment)



(d) Circular Deformation (Analysis)

Fig. 7 Time Variation of Deformations

deformation is defined as the average values of deformations in x, y direction of 4 corners ($a_{x(y)}$, $b_{x(y)}$, $c_{x(y)}$, $d_{x(y)}$ in Fig. 6). It is considered to have similar behavior with inner expansive mortar and is representative for the inner motion of the expansive mortar. Thus, uniform deformation is chosen as the basis for comparison. Circular deformation is defined as the difference between the maximum and the uniform deformation (difference between the average of maximum deformations in 4 profiles and the average uniform deformation).

Thus, comparison is presented in Fig. 7. Fig. 7-(a) and (b) are the uniform deformation for experiment and analysis; while Fig. 7-(c) and (d) are the comparison for circular deformation. The data of experiment is the average values of section 2~4 shown in Fig. 1. As illustrated in Fig. 7-(a), the uniform deformation from experiment increases slowly before the first 8 hours (0 hour is defined as the time point when the expansive mortar has just been cast into the specimen); thus, due to the occurrence of penetrating cracks in corners (refer to Fig. 10), a drastic increasing occurs during 8 to 12 hours; correspondingly, the circular deformation of experiment (Fig. 7-(c)) also has a intense increasing during this time interval; after that, as decrease of reaction speed for expansive mortar (crack conditions in concrete surface are also confirmed to have small variation after 12 hours), the deformation value becomes to converge with maximum as 3.32mm.

Temperatures are input linearly into the expansive mortar in analysis. Therefore, as presented in Fig. 7-(b), the variation of deformation from analysis increases almost linearly until to the maximum as 2.71mm when divergence occurs in 261st step. This final step of analysis with closest value to maximum of experiment is chosen to compare with the ultimate of experiment. In this stage (S2 of Fig. 7-(a), (b)), the uniform deformation is 3.32mm in 24 hours and 2.71mm in 261st step for experiment and analysis, respectively. Further, another stage (S1 of Fig. 7-(a), (b)) is chosen with uniform deformation as 1.48mm and 1.36mm being almost half of the maximum for experiment and analysis, respectively.

As illustrated in Fig. 7-(c) and (d), the circular deformation in S2 is 4.04mm and 5.00mm for experiment and analysis; the ratio of circular to uniform deformation is 1.49 for analysis similar to 1.51 for experiment. For S1, the circular deformation is 2.87mm and 2.76mm for experiment and analysis; also the ratio of circular and uniform deformation is 1.86 close to 1.94 of experiment.

Fig. 8 presents the general deformation shape of experiment for stage S2 of Fig. 7-(a). It is observed that the maximum values

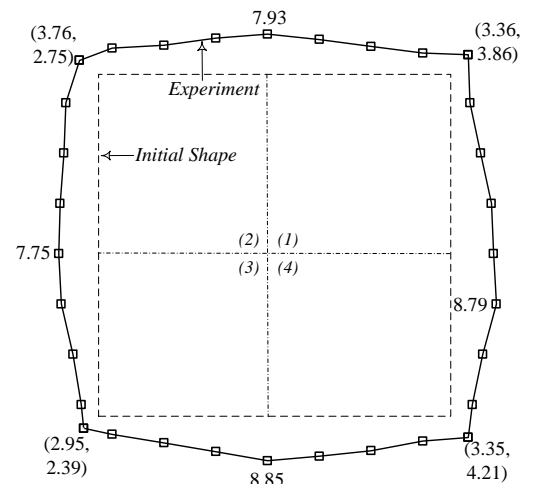


Fig. 8 Deformations in S2 (Experiment)

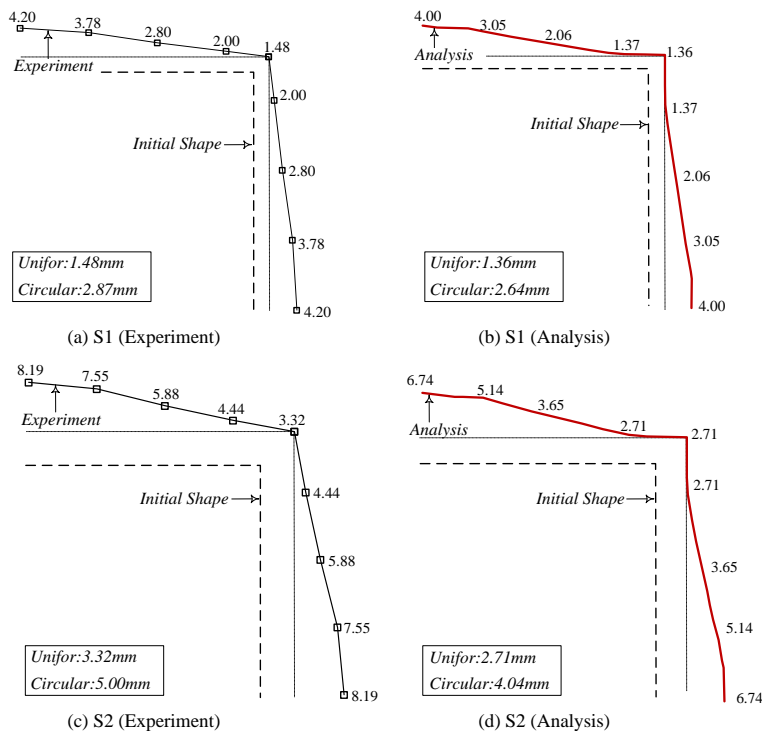
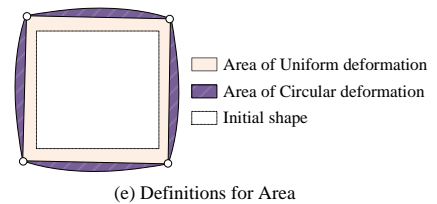
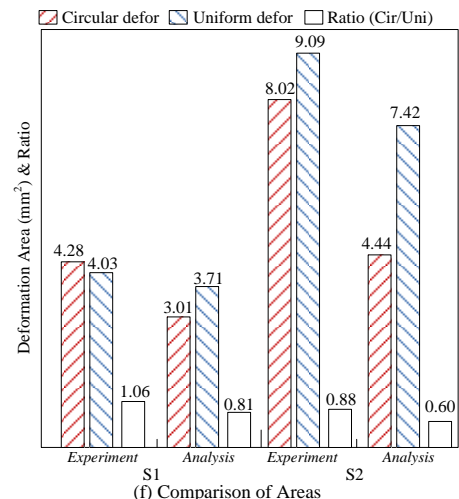


Fig. 9 Comparison of Deformation Shapes



(e) Definitions for Area



(f) Comparison of Areas

in profile changes from 7.75mm to 8.85mm; while values in corners varies from 2.39mm to 4.21mm. For detailed comparison with analysis, 1/4 of the deformation shape is used by averaging the corresponding values in four quadrants ((1)~(4) of Fig. 8).

Fig. 9 shows the comparison of deformation shapes. From Fig. 9-(a)~(d), the deformation in center of profile is greater than that in corner. Combined with descriptions in Fig. 7, it is concluded that the circular deformation is verified for both experiment and analysis. Further, the circular deformation is also confirmed in the specimen using reactive aggregates from former research⁶⁾.

The deformation area is also compared. As shown in Fig. 9-(e), deformation area is divided by two parts. One is the area of uniform deformation as increasing of the quadrilateral connecting four corner points; another part is the area of circular deformation which is the difference between total area and area of uniform deformation. As presented in Fig. 9-(f), the area of uniform deformation for analysis is in smaller level due to the smaller final uniform deformation (2.71mm, Fig. 7-(b)). Concentrating on the ratio between area of circular and uniform deformation, the trend of area for circular deformation is weaker in analysis. The possible reason will be evaluated in the next section.

3.2 Crack Conditions

In this section, the crack conditions will be compared. Fig. 10 illustrates cracks in upper section of experiment in stage S2. After the end of expansion, the inner section of specimen has been cut off and similar crack form to that in upper section is confirmed. Thus, the crack conditions in upper section are used for representative. Cracks are measured by scale and sketched together with the progress of expansion. Crack with the width greater than 0.05mm is selected as the objective. It is observed that cracks have greater width in corner area with the maximum as 4.0mm. However, those in central area have relatively small width. It can be summarized that there are two main styles of cracks occurred during the expansion: crack in central area (A of Fig. 10) develops from the profile and cracks in corner area (B of Fig. 10) from the inner expansive mortar with the direction around 45°.

Fig. 11 illustrates the definition of cracks in analysis⁷⁾. In the direction perpendicular to maximum principal strain with values greater than cracking strain (177μ, Fig. 3), the crack is defined to occur. The crack width is defined as the product of strain and equivalent length (L of Fig. 11, determined as 10mm based on element size).

For cracks in corner area, Fig. 12 presents the vector distributions of maximum principal strain with value greater than cracking strain. It is known that great strains occur in corner area with the crack position roughly coincide with that in experiment. As to detailed evaluation, the maximum strain as 0.215 is generated in the boundary between expansive mortar and frame concrete. Translating to crack width, it is 2.15mm (0.215×10mm) with similar level to that in experiment. Further, different with experiment, the crack in analysis is not penetrating the corner part. This will give more restraint to the occurrence of circular deformation which corresponds to the smaller trend for area of circular deformation in analysis (Fig. 9-(f)).

Besides, as illustrated in Fig. 12, greater strain as 0.023 (yield strain as 0.0019, Fig. 3) occurs in the inner bent part of stirrup. It is estimated that the circular deformation of external concrete can lead to the opening deformation of stirrup (increase of angular degree in bent part of stirrup)²⁾. Therefore, the greater strain in bent part of stirrup is considered to be caused by the opening deformation. Further, this great strain will increase the possibility to the progress of initial damage in stirrup and even the rupture of stirrup, which is confirmed to occur in section 2 and 5 of specimen as shown in Fig. 1 and detailedly described in reference²⁾.

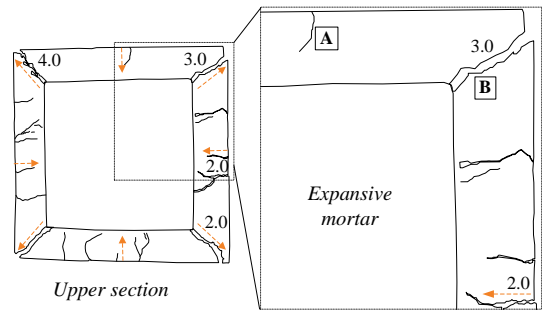


Fig. 10 Crack Conditions (Experiment)

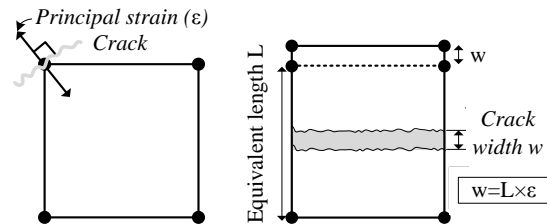


Fig. 11 Definition for Crack Direction & Width

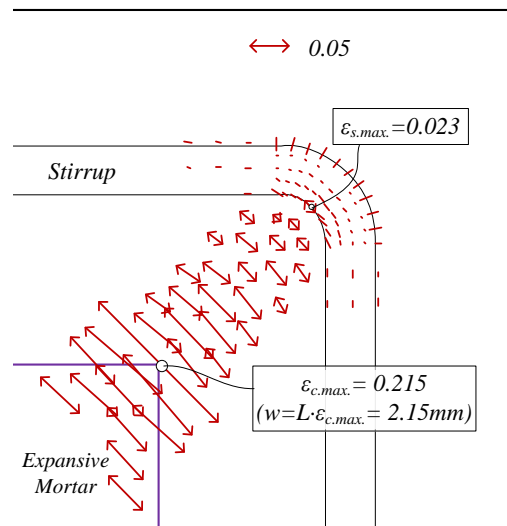


Fig. 12 Strain in Corner Part

Fig. 13 presents the enlarging of strains in central part. As shown in zone *p*, from upper to inner side, the strain decreases from 0.162 to 0.064, this infers the occurrence of cracks in center surfers the contribution from bending effect. Further, 5 lines with the spacing near 30mm are selected to investigate the strain distribution in cross-section of frame concrete. As illustrated in Fig. 13, the strain greater than crack strain is summed up (Sum_1 as 0.307, Sum_5 as 0.131 for instance).

Therefore, Fig. 14 shows the strain distributions based on the strain measurements illustrated in Fig. 13. The strain distributes in ladder-shape. The neutral axis is assumed to locate in 89.6mm from upper side (0.8 times of cross-section, confirmed by sectional calculation). Thus, the strain caused by uniform tension is calculated as 0.166 (width as 1.66mm) and by bending effect is 0.141 (width as 1.41mm). The circular deformation of external concrete is considered to be caused by this bending effect. The calculated width from uniform tension is 1.66mm as around 61% of the uniform deformation (2.71mm, Fig. 7-(b)). This means the uniform deformation in analysis is mainly caused by the component of uniform tension from cracks in central part. However, from the crack conditions of experiment in Fig. 10, the uniform deformation in experiment is estimated to suffer more influence from penetrating cracks of corner parts.

4. CONCLUSIONS

- (1) From the results of experiment and analysis, the maximum deformation in center of profiles is greater than those in corner. The ASR-induced circular deformation is reproduced by both the analysis and experiment;
- (2) It is estimated that the circular deformation can lead to the opening deformation of stirrup. Therefore, great strain as 0.023 occurs in bent part of stirrup. This will promote the progress of initial damage, which will further cause rapture of stirrup as confirmed by experiment.
- (3) From distributions of maximum principal strain, the crack positions from analysis can coincide with experiment; based on analysis, the circular deformation is caused by the component of bending effect and uniform deformation is mainly caused by the component of uniform tension effect in central cracks;

REFERENCES

- 1) JSCE: *Report of Committee for ASR Countermeasures -Fracture of Rebar and New Correspondence*, Concrete Library, No. 124, pp.1-2~1-77, 2005
- 2) Kosa, K., and Kusano, M.: *Evaluation of Deterioration Using an ASR-imitated Test Specimen*, Journal of JSCE, Ser. E2 (Materials and Concrete Structures) Vol. 69, No. 2, pp. 166-181, 2013
- 3) Koroki, N., and Kosa, K.: "Influence from Rib Shape and Expansion of Concrete on Stirrup Fracture," *Proceedings of the Japan Concrete Institute*, Vol.28, No.1, pp. 719-724, 2006
- 4) Ueda, N., and Sawabe, S.: *Analytical Study on The Expansion Induced by Alkali Silica Reaction for RC Members*, Journal of JSCE, Vol. 63, No. 4, pp. 532-548, 2007
- 5) Nishigori, T.: *Construction of Steel Lined Penstock due to Expansive Cement Concrete*, Concrete Journal, Vol. 12, No. 7, pp. 35-50, 1974
- 6) Kusano, M., and Kosa, K.: "Evaluation for Progress of Stirrup Damages Using ASR Specimens," *Proceedings of the Japan Concrete Institute*, Vol.33, No.1, pp. 989-994, 2011
- 7) Sato, T., and Kosa, K.: "Detailed Damage Analysis of Footing due to Seismic Load," *Journal of Structural Engineering*, Vol. 60A, pp. 923-935, 2014

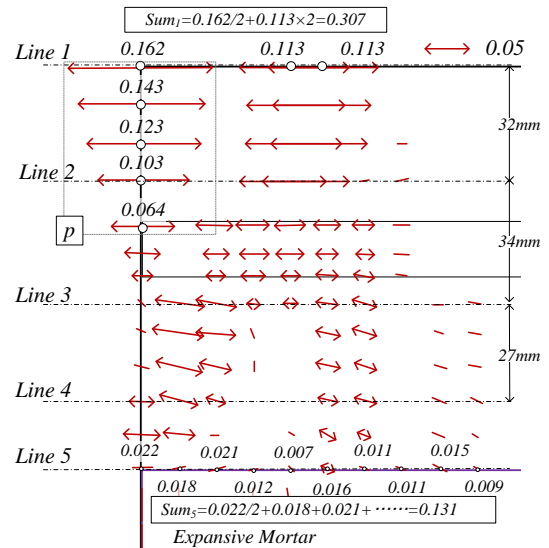


Fig. 13 Strain in Central Part

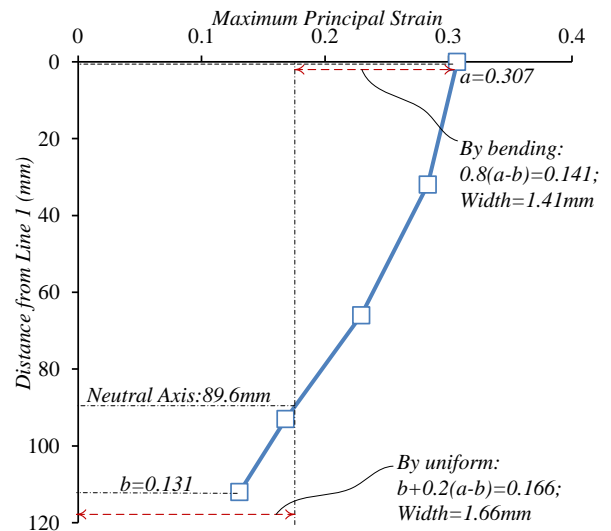


Fig. 14 Generate of Uniform Deformation